ACOUSTICS OF A BACKWARD CURVED RADIAL FAN – CAA SIMULATION AND EXPERIMENTAL VALIDATION

Andreas LUCIUS[1], Rebecca SCHÄFER[2],

[1] *ebm-papst Mulfingen GmbH & Co. KG, Bachmühle 2,*
74673 Mulfingen, Germany,

[2] *Institute of Fluid Mechanics and Turbomachinery TU Kaiserslautern,*
Gottlieb-Daimler Straße G 44,
67663 Kaiserslautern,, Germany

SUMMARY

For detailed analysis of sound generation mechanisms in low speed fans, CAA simulations are a key technology. For industrial purpose, high quality Large Eddy Simulations (LES) are not feasible. In addition periodic simulations of single blade channels offer further potential to reduce computational costs. In this paper a radial fan configuration with and without spiral casing was analyzed numerically with CAA simulations. The influence of the computational grid was studied for single blade periodic model, which showed satisfactory results at a moderate cell count. A comparison with the full rotor simulation showed differences especially at microphone positions out of the rotational axis and at low frequencies. The differences are attributed to coherent sound in the case of periodic model. The influence of the spiral casing on sound power was well predicted in simulations.

INTRODUCTION

For detailed understanding of sound generation mechanisms in low speed fans, simulation techniques are increasingly used. This insight helps to design low noise fans. A variety of methods is used to solve this problem. The most common "hybrid" approach solves the flow field with CFD and applies an analogy for the acoustic field. As turbulent fluctuations are essential for the noise generation, scale resolving turbulence models such as Large Eddy Simulations (LES), or Detached Eddy Simulations (DES) are needed. A good example for the variety of simulation techniques is the axial fan with a diameter of 300 mm experimentally analyzed in detail in Siegen by Carolus *et al*. [1]. The main noise generation mechanisms investigated were blade tip noise and the influence of inflow turbulence. For this benchmark a number of research groups applied different numerical

methods for CAA simulations. High quality LES for the CFD coupled with a Discontinuous Galerkin solver for the APE equations was used by Pogorelov *et al*. [2]. Simulations with LES and FW-H (Ffowcs-Williams and Hawkings) propagation for the acoustics were presented by Dietrich *et al*. [3]. In this study coarse grid LES feasible in industrial context was applied for different tip gaps. The influence of tip clearance was captured with reasonable accuracy. The Lattice Boltzmann Method (LBM) has also been applied successfully for this test case by Zhu and Carolus [4]. Sturm *et al*. [5] showed, that a detailed representation of the acoustic test rig is needed to capture the tonal noise due to asymmetry of the incoming flow field. Liberson *et al*. [6] used synthetic sources in the tip gap region based on the RANS mean flow field. This approach avoids the time consuming effort of resolving the turbulent sources in the flow simulation. The results showed some deviations in the mid frequency range, which were attributed to anisotropic effects [7]. Further efforts are needed to include this effect. Synthetic turbulence was also used by Dietrich and Schneider [8] and Alavi Moghadam [9] to model the effect of inflow turbulence. The increase of broadband noise at low frequencies was lower compared to experiment in [9]. This was attributed to the assumption of isotropic turbulence for the generated turbulence and circumferential averaging needed for the periodic single blade simulations. Dietrich and Schneider [8] showed that using circumferential averaging of the RANS field as input for turbulence reconstruction leads to lower broad band noise predictions in the low frequencies.

In this paper, we focus on a radial fan with low Mach number flow. All the methods listed above are also applicable. Some of these simulations used periodic models of a single blade channel [2], [3], [8], [9], resulting in coherent sources. Results were promising, but the influence of coherence of the resulting sound field was not discussed in these studies. We will show that coherence has an effect on the results. It needs to be considered for comparison with measurements.

FAN CONFIGURATION AND EXPERIMENTAL SETUP

The validation test case is a backward curved centrifugal fan with a diameter of 190 mm designed by ebm-papst Mulfingen GmbH & Co. KG. The fan was measured in the suction side chamber fan test rig in the anechoic room of the Institute of Fluid Mechanics and Fluid Machinery at the University of Kaiserslautern, results are published by Schäfer and Böhle [10]. The design rotational speed was 3635 rpm, test rig is designed according to DIN EN ISO 5801. The sound pressure was measured at 11 positions on a hemisphere at the pressure side of the fan. Two different configurations were analyzed: the fan alone and the fan with a spiral casing. The casing was made of acrylic glas, in order to have optical access. Measurements in that project were used for validation of CAA simulation with the LBM code Powerflow. The simulation results showed very good agreement to measurements [10]. In a recent investigation by Schäfer [11] numerical efforts could be reduced by 80 % from 37.600 CPUh to 7700 CPUh with acceptable loss in accuracy.

COMPUTATIONAL MODEL

In this investigation both configurations - with and without spiral casing - were simulated. For all simulations the general purpose CFD solver StarCCM+ version 14.04-r8 was applied. All configurations were run as compressible Large Eddy Simulations using the WALE subgrid model. The aeroacoustics was evaluated using the pressure at specific microphone positions. The FW-H method is only applicable for the fan alone. For the case with spiral casing, a free field radiation from the impeller is no valid assumption. Permeable FW-H emission surfaces are difficult to apply for microphones on the pressure side. This approach is valid only for the propagation of acoustic pressure fluctuations into the far field. If the emission surface is placed in turbulent flow, hydrodynamic fluctuations are propagated to the far field. As the distance to the microphones is comparably small, direct evaluation is feasible. The grid in the acoustic evaluation region, in which all microphones are placed, is resolved with 16 mm cell size for the coarse grid and 12 mm for the fine grid. This corresponds to 10 respectively 15 points per wavelength for a target frequency

of 2000 Hz. Typically ~ 20 points per wavelength are needed for second order differencing schemes [12]. Here we apply a third order MUSCL scheme for the spatial discretization of the convective terms. This scheme blends third order upwind with third order central differences, a blending factor of 0.15 was chosen. The results show higher cut-off frequency as will be shown later. The influence of the computational grid was initially studied for the case without spiral casing. For this setup, the inflow chamber was modified to round cross section with the same area compared to the rectangular chamber in the measurements as shown in Figure 1. This simplification allows the application of a periodic model. This change may effect the acoustic emissions. Corner vortices are expected in case of the rectangular chamber. The influence of the suction side chamber on fan alone configuration was not studied. For the second configuration with casing, the inlet chamber was modelled as measured. Figure 1 shows the different setups with the grid refinement for acoustic propagation. All far field boundaries were set to non-reflecting free stream conditions. The required Mach number and pressure distributions were taken from an initial RANS solution.
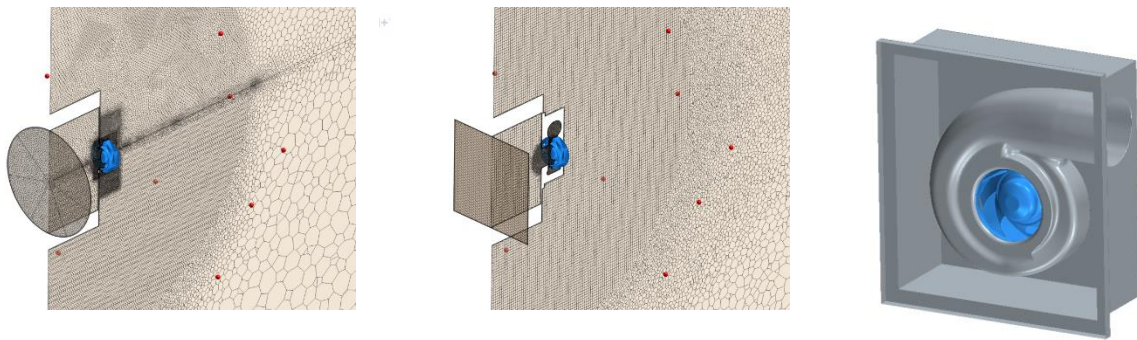

Figure 1: computational model with coarse mesh, left fan alone, mid and right full model with casing

We evaluated the periodic model for two computational grids. Table 1 shows the cell count for all different configurations. The cell count applied is much coarser compared to high quality LES published by Pogorelov *et al*. [2]. The boundary layer was resolved in wall normal direction with y^+ less than 1 for most of the impeller. The non-dimensional cell size on the wall x^+ is calculated from the area of the unstructured polyhedral cell on the surface. Maximum x^+ at design point is 300 for the coarse grid and 250 for the fine, with mean values of 108 and 87 respectively. The full model mesh contains identical patterns of the periodic setup to allow mesh independent comparison of full model and periodic results.

The time step was chosen to resolve a single blade passage with 400 time steps ($\Delta t \sim 1.1e\text{-}5$ s). This corresponds to 80 steps per period at 2000 Hz. A second order backward scheme was applied for temporal discretization.

Table 1: cell count and computational effort for different configurations

Configuration	CFD setup	Cell count [mio]	Cell size acoustic evaluation [mm]	CPUh
Fan alone	**Periodic coarse**	1.4	16.0	780
	Periodic fine	2.7	12.0	1500
	Full coarse	9.8	16.0	8000
Fan with casing	**Full coarse**	9.1	16.0	8000

The simulation procedure is always the following. After an initial RANS three revolutions were simulated with a coarse time step (50 steps per blade passage) to convect initial disturbances. For the final evaluation of the aeroacoustics, 10 revolutions with the fine time step were computed,

which corresponds to 0.165 seconds. The total CPUh for the computations are also listed in Table 1. For the simulation with casing some more initial time was needed to reach the correct operating point. The larger simulations were done on the HLRS Supercomputer of the University in Stuttgart with up to 640 cores. The low cell counts lead to feasible turn-around times of 12 hours for the full model simulations.

PERIODIC VERSUS FULL MODEL SIMULATIONS – FAN ALONE

As pointed out in the previous section, the reduction to periodic models of a single blade results in a strong reduction of computational effort. This method was applied successfully for an axial fan [2], [3], [8], [9]. There are some known limitations of this approach: it is only applicable for rotational symmetric configurations and for stationary flow conditions. Especially at low flow rates with massive flow separation the assumption of periodic flow in each blade passage may be violated. Flow phenomena as rotating stall cannot be treated with periodic models.

The focus of this section is the influence of coherent sound sources on the results. In experiment, the small scale turbulent fluctuations on adjacent blade channels can be assumed to be uncorrelated. The same is true for a full model Large Eddy Simulation. All single blades are independent sound sources, as the fluctuating forces are different on each blade in every time step. A periodic model results in exactly the same fluctuation forces on every single blade, which results in coherent sound sources. For microphones on the axis of rotation, coherent sound from all blades arrives at exactly the same phase angle. This leads to over prediction of Δ SPL = 10.0 log (z) dB compared to measurements. Here SPL is the sound pressure level and z the number of blades. This type of correction is also applied in [8]. The spectra in Figure 2 show the comparison of the power spectral density (PSD) of microphone 10 on the axis and mic 8 off the axis at a distance to the fan of 1m. Frequency resolution Δf is ~42 Hz in simulations, corresponding to 10 steps per blade passing frequency (BPF). Experimental resolution is 6.25 Hz. The left diagrams in Figure 2 show spectra at 70 % of max. efficiency flow rat Q_{opt}, the diagrams on the right side display results at Q_{opt}. On the axis (top diagram) the spectra are corrected for the periodic model. Full model and periodic model match very well and are close to experiments. For the microphones off the axis (middle diagram), no correction is applied. The distance of every individual blade to the microphone is different, resulting in a phase shift. The spectra at microphones off axis show an over prediction for the periodic simulations of ~ 5 to10 dB at frequencies below 300 Hz. The full model with identical mesh shows good agreement to measurements. Low frequency humps at 300 Hz and 650 Hz due to separation on the blade at part load are captured in periodic as well as full simulation. The periodic simulation results show two additional peaks at 800 and 1200 Hz off axis. These peaks are also found in measurements on the axis. The periodic setup seems to amplify them off axis. For the design operating point similar effects are observed. A deviation of periodic and full model is found at low frequencies off axis, on axis the simulated spectra show a constant shift of ~ 10.0 log (7) = 8.5 dB.

All pictures indicate a minor difference concerning grid resolution. One sharp peak at 2500 Hz appears only for the coarse grid periodic simulation at 100 % flow rate. It is not found in the refined periodic simulation. For all simulations the cut-off in the simulated spectra is higher than the 2000 Hz target. A good agreement up to 3 kHz is found. For overall levels spectra in the range of 100 to 3000 Hz are considered (lower diagrams in Figure 2). The deviations in the low frequency range due to periodic effects leads to over prediction of the overall sound pressure especially in microphone 8 and 9. The sound power level (SWL) is 2-3 dB higher for periodic simulations. For the full rotor setup all microphones are predicted with less than 2 dB error. The sound power is derived as the average overall level of all microphones and a half sphere as integration surface. The deviation in sound power is in the range of 1 dB for the full model simulations.
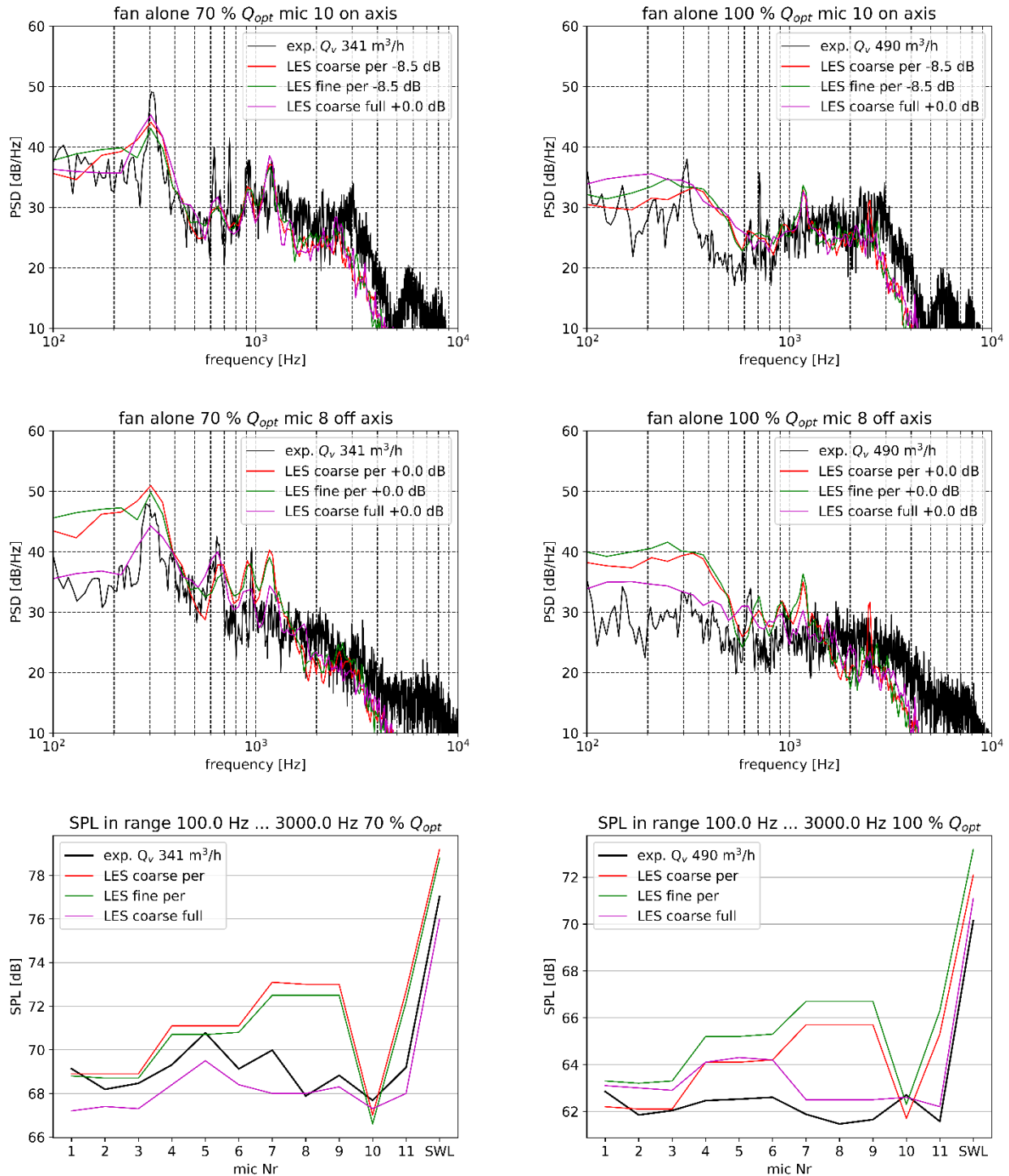
Figure 2: sound pressure spectra and overall levels, left 70 % Q_{opt}, right 100 % Q_{opt}, top mic10 on axis, mid mic 8 off axis, bottom overall sound pressure level

For a further investigation of the influence of coherent sound emission, the sound pressure at additional microphones on a half circle with distance 1 m to the fan was recorded. For all microphones, the difference of the sound pressure spectrum between full model and periodic simulation was calculated. For visualization purpose the spectra were integrated to octave bands. Figure 3 shows the Δ SPL depending on directivity respectively distance to the axis and frequency. The difference corresponds approximately to the correction -8.5 dB for every frequency on the axis of rotation. There are some deviations for the very low frequencies at the design point shown in the right diagram. For the higher frequencies, the difference between coherent and not coherent sound

is limited to positions close to the axis of rotation. At higher directivity angles the difference approaches zero. For lower frequencies the influence of coherence is not limited to the axis, but also seen at larger distance. The lower the frequency, the larger is the region of influence of coherent sound.

There is a high positive difference for 2 kHz octave band. This effect is probably not an effect of coherence of sound, but due to limitations of capturing the correct sources in the periodic simulations. The lower diagrams of Figure 3 display the spectra at microphone 2, which corresponds to 80 degree. The full model simulations as well as experiments show a hump at 2000 Hz, which is not captured for the periodic simulations. Another effect is seen for the 500 Hz band for the 70 % part load case. The periodic model cannot resolve the hump between 600 and 700 Hz as well.

Further investigation is needed and will be conducted regarding the comparison of acoustic sources for periodic and full rotor simulations in terms of surface pressure spectra.
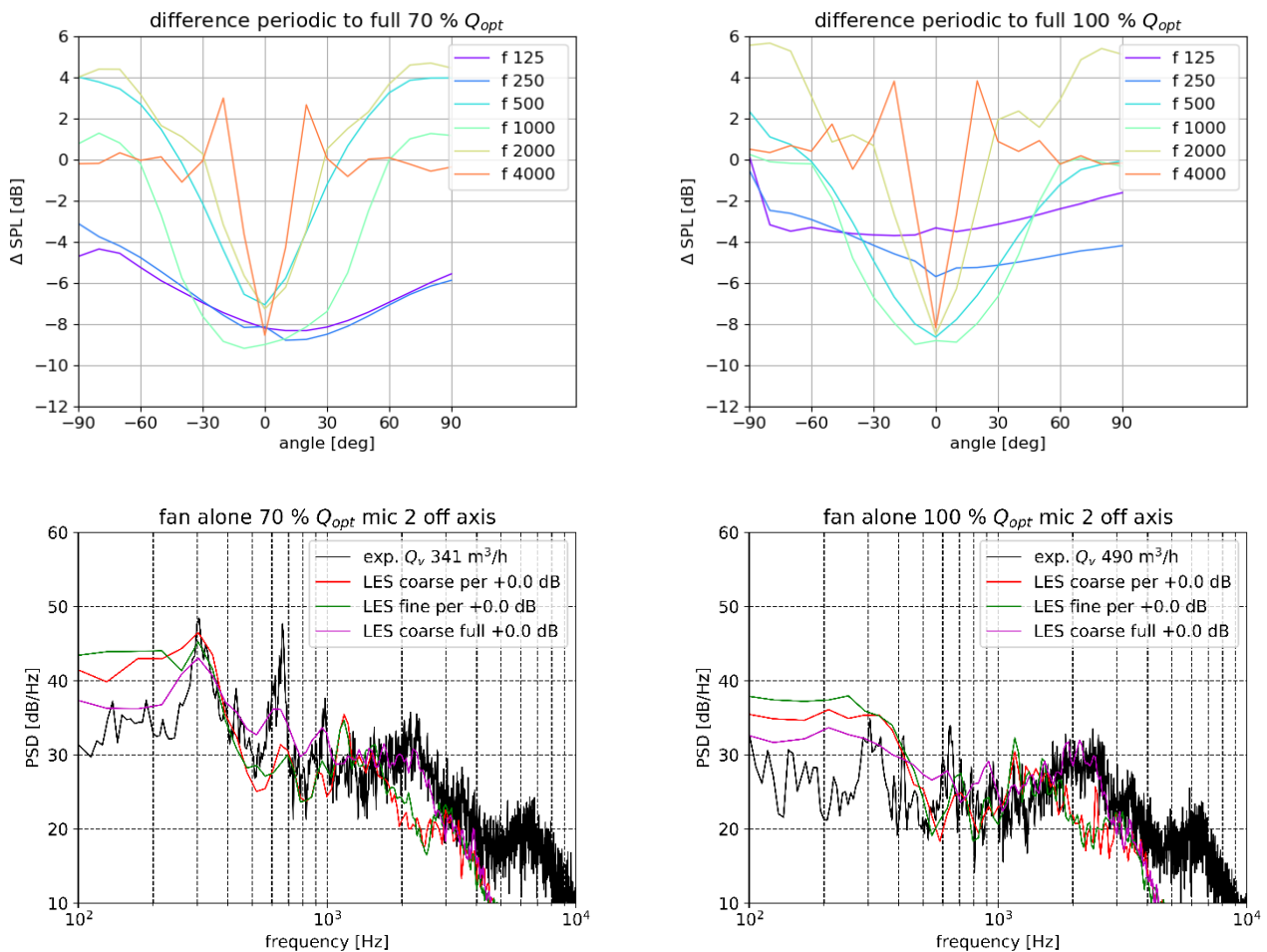
Figure 3: top difference in octave band levels between periodic and full model simulations,
(left) 70 % Q_{opt} (right) 100 % Q_{opt}, bottom spectra at directivity angle 80 degree

FAN WITH AND WITHOUT CASING

In the following, the influence of the spiral casing on the acoustic emission is analyzed. There is a shift of the flowrate at Q_{opt} to lower values for the configuration with casing. Figures 4 and 5 show the influence of the spiral casing on sound emission and propagation. Due to rotor-stator interaction, especially with the volute tongue, the sound pressure level at blade passing frequency (BPF ~ 420 Hz) is strongly increased. The frequency resolution in simulation was increased to 20 points per BPF compared to the results shown in the previous section. The tonal noise peak at BPF is found, but with lower peak amplitude and not as sharp as in the measurements. The simulation time of 10 revolutions for evaluations (0.12 sec) is too short for a resolution in frequency compared to experiments. The prediction of tonal noise is a demanding task for the simulation in terms of computational effort. There is also broadband increase at low frequencies but also some decrease in higher frequencies. Figure 4 shows the comparison of simulated and measured spectra for design point and part load for two different microphone positions. For both simulation cases the full model results are shown. The differences due to the spiral casing are very well predicted for both operating points. At low frequencies broad band noise increases. Destructive interference at 1200 Hz in the propagation with spiral casing well captured in simulation.
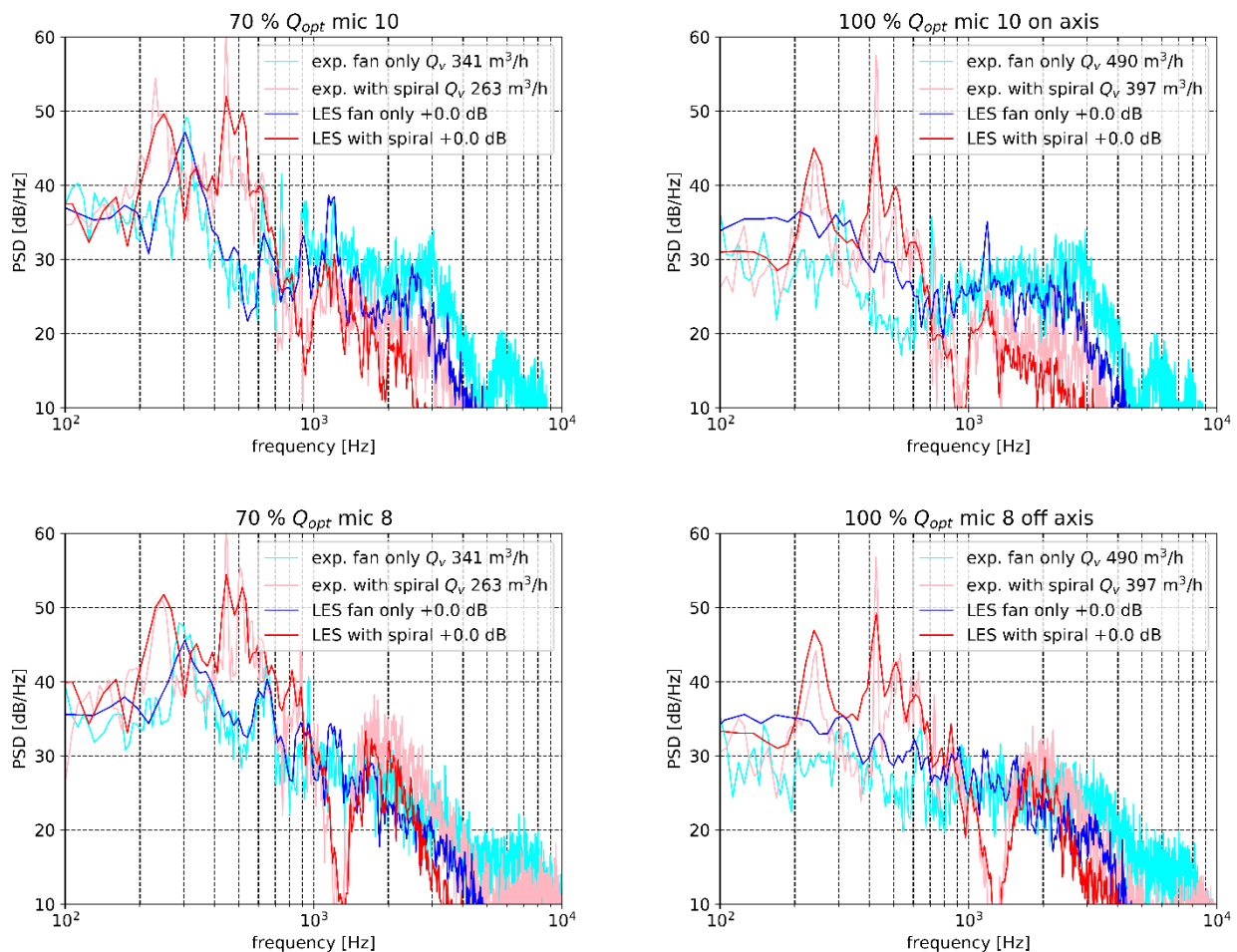

Figure 4: sound pressure spectra with and without spiral casing, (left) 70 % Q_{opt}, (right) 100 % Q_{opt} top mic 10 on axis, bottom mic 8 off axis
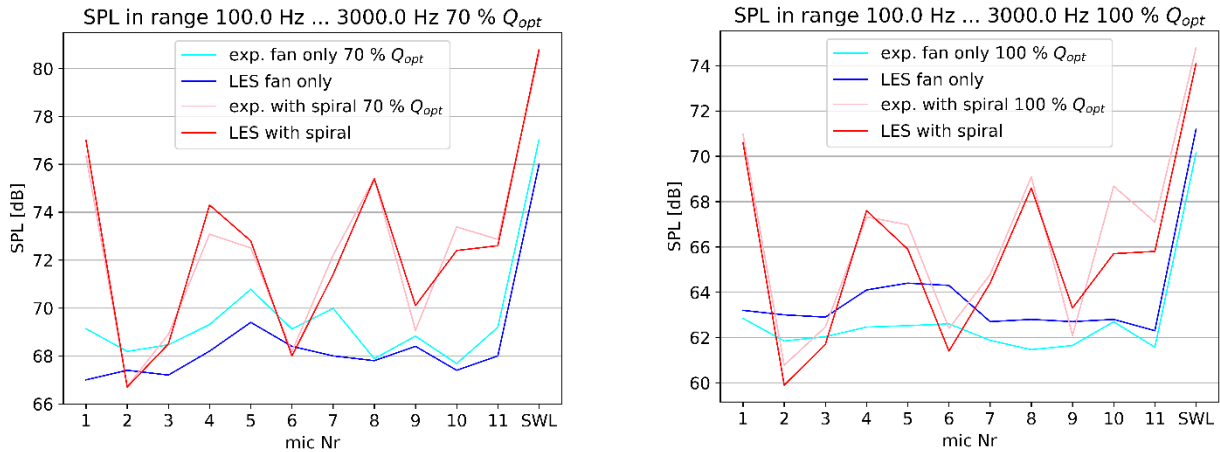
Figure 5: overall sound pressure levels with and without spiral casing, (left) 70% Q_{opt}, (right) 100 % Q_{opt}

Figure 6 shows the integral performance for the fan alone versus the fan with casing. The spiral casing increases pressure rise at low flow rates, but decreases the maximum flow rate. The trends were captured well in simulations, but both cases were over predicted. The reason for the deviation is probably the size of the acoustic chamber, resulting in difference in static pressure recovery. The simulations contains free outlet with a distance of 2.5 m from the fan. The chamber is smaller in experiment. For the fan alone periodic and full rotor simulation results are almost identical.

The sound power strongly increases for the fan with spiral casing, especially at high flow rates. For proper comparison with simulations, the sound power only contains the frequencies between 100 and 3000 Hz. As already indicated in Figure 2 and Figure 4 sound power is in very good agreement for all operating points. The large differences in sound power between both configurations are predicted at high accuracy with full model simulations. The deviation is less than 2 dB for all operating points. The periodic simulation resulted in larger errors of sound power, especially at 70 % Q_{opt}. The reason is the increase of levels due to coherence. On the axis of rotation the influence can be corrected with a constant shift of levels, off the axis a correction depending on frequency and position is needed.
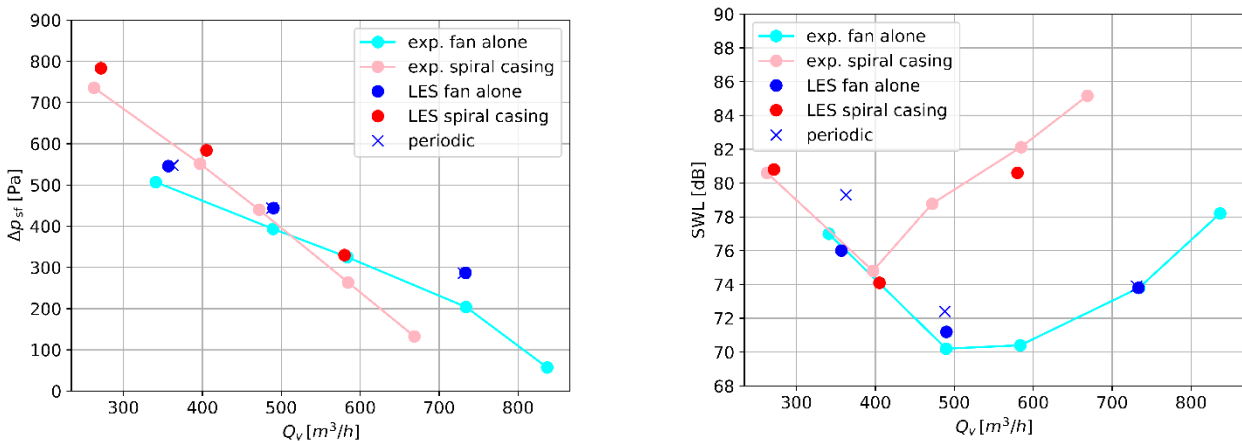

Figure 6: integral performance, (left) pressure rise, (right) sound power outlet

CONCLUSIONS

In this investigation, aeroacoustic simulations with a commercial CFD solver were done for a radial fan with and without casing. Direct evaluation of the compressible pressure at microphone positions was used for the acoustic field. The results showed good agreement with measurements, despite the low resolution around the fan blades and in the acoustic field. Especially the cut-off frequency was much higher than expected for a CFD solver. Spectra were in reasonable agreement to measurements with less than 10 points per wavelength. It was shown, that periodic simulations can

be used to predict sound pressure spectra on the rotational axis for a wide range of flow rates. The spectra at microphone positions off axis show deviation in far field acoustics between full rotor and periodic simulations. This deviation depends on position and frequency. Further investigation is needed regarding the influence of periodicity on the sources. This error mainly influences the prediction of absolute levels in comparison to measurements. It is expected, that trends between different fan designs can be derived from comparably cheap single blade computations.

BIBLIOGRAPHY

[1]   T. Carolus, T. Zhu, M. Sturm – *A low pressure axial fan for benchmarking predictions for aerodynamic performance and sound*, Noise Control Engineering Journal, 63 (6), **2015**

[2]   A. Pogorelov, M. Meinke, W. Schröder – *Impact of periodic boundary conditions on the flow field an in axial fan* AIAA Paper 2016-0610, **2016**

[3]   P. Dietrich, A. Lucius, M. Schneider – *Einfluss der Kopfspaltgröße auf die Aeroakustik von Axialventilatoren,* Proceedings of the DAGA 2017 Kiel, **2017**

[4]   T Zhu, T. Carolus – *Experimental and numerical investigation of tip clearance noise of an axial fan using a Lattice Boltzmann Method,* Proceedings of the fan 2015 International Conference, Lyon, **2015**

[5]   M. Sturm, M. Sanjosé, S. Moreau, T. Carolus – *Aeroacoustic simulation of an axial fan including the full test rig by using the Lattice Boltzman Method*, Proceedings of the fan 2015 International Conference, Lyon, **2015**

[6]   L. Liberson, M. Lummer, M. Mößner, R. Ewert, J.W. Delfs – *Application of a Discountinuous Galerkin based CAA solver for broadband noise prediction*, Proceedings of the fan 2018 International Conference, Darmstadt, **2018**

[7]   L. Liberson, M. Lummer, M. Mößner, R. Ewert, J.W. Delfs – *Axial Ventilator Tip Gap Noise Prediction from Discontinuous Galerkin based CAA with Stochastic Vortex Sound Sources*, Proceedings of the 23rd International Congress on Acoustics, **2019**

[8]   P. Dietrich, M. Schneider – *Aeroacoustic Simulations of an axial fan with modelled turbulent inflow conditions,* Proposed Proceedings of the fan 2022 International Conference 2022 Senlis, **2022**

[9]   S.M. Alavi Moghadam, A. Pogorelov, B. Roidl, M. Meinke, W. Schröder – *Numerical Analysis of the Acoustic Field on an Axial Fan at Varying Inflow Conditions,* Proceedings of the fan 2018 International Conference, Darmstadt, **2018**

[10]   R. Schäfer, M. Böhle – *Validation of the Lattice Boltzmann Method for Simulation of Aerodynamics and Aeroacoustics in a Centrifugal Fan,* Acoustics 2(4), **2020**

[11]   R. Schäfer – *Optimierung der LB Simulation eines Radialventilators hinsichtlich des Rechenaufwand,* Abschlussbericht FLT Vorhaben L269, **2021**

[12]   C. Tam – *Computational Aeroacoustics,* Cambridge University Press, **2012**